Investigating the chemical species in submicron particles emitted by city buses

Saarikoski, S.

2017

Saarikoski , S , Timonen , H , Carbone , S , Kuuluvainen , H , Niemi , J V , Kousa , A , Rönkkö , T , Worsnop , D , Hillamo , R & Pirjola , L 2017 , ' Investigating the chemical species in submicron particles emitted by city buses ' , Aerosol Science and Technology , vol. 51 , no. 3 , pp. 317-329 . https://doi.org/10.1080/02786826.2016.1261992

http://hdl.handle.net/10138/308153
https://doi.org/10.1080/02786826.2016.1261992

Aerosol Science and Technology

ISSN: 0278-6826 (Print) 1521-7388 (Online) Journal homepage: https://www.tandfonline.com/loi/uast20

Investigating the chemical species in submicron particles emitted by city buses

S. Saarikoski, H. Timonen, S. Carbone, H. Kuuluvainen, J. V. Niemi, A. Kousa, T. Rönkkö, D. Worsnop, R. Hillamo & L. Pirjola

To cite this article: S. Saarikoski, H. Timonen, S. Carbone, H. Kuuluvainen, J. V. Niemi, A. Kousa, T. Rönkkö, D. Worsnop, R. Hillamo & L. Pirjola (2017) Investigating the chemical species in submicron particles emitted by city buses, Aerosol Science and Technology, 51:3, 317-329, DOI: 10.1080/02786826.2016.1261992

To link to this article: https://doi.org/10.1080/02786826.2016.1261992

AEROSOL SCIENCE AND TECHNOLOGY
2017, VOL. 51, NO. 3, 317–329
http://dx.doi.org/10.1080/02786826.2016.1261992

Taylor & Francis
Taylor & Francis Group

Investigating the chemical species in submicron particles emitted by city buses

S. Saarikoski[a], H. Timonen[a], S. Carbone[a,*], H. Kuuluvainen[b], J. V. Niemi[c,d], A. Kousa[c], T. Rönkkö[b], D. Worsnop[e,f], R. Hillamo[a], and L. Pirjola[f,g]

[a]Air Quality, Finnish Meteorological Institute, Helsinki, Finland; [b]Aerosol Physics Laboratory, Department of Physics, Tampere University of Technology, Tampere, Finland; [c]Helsinki Region Environmental Services Authority HSY, Helsinki, Finland; [d]Department of Environmental Sciences, University of Helsinki, Helsinki, Finland; [e]Aerodyne Research, Inc., Billerica, Massachusetts, USA; [f]Department of Physics, University of Helsinki, Helsinki, Finland; [g]Department of Technology, Metropolia University of Applied Sciences, Helsinki, Finland

ABSTRACT

Detailed chemical characterization of exhaust particles from 23 individual city buses was performed in Helsinki, Finland. Investigated buses represented different technologies in terms of engines, exhaust after-treatment systems (e.g., diesel particulate filter, selective catalytic reduction, and three-way catalyst) and fuels (diesel, diesel-electric (hybrid), ethanol, and compressed natural gas). Regarding emission standards, the buses operated at EURO III, EURO IV, and EEV (enhanced environmentally friendly vehicle) emission levels. The chemical composition of exhaust particles was determined by using a soot particle aerosol mass spectrometer (SP-AMS). Based on the SP-AMS results, the bus emission particles were dominated by organics and refractory black carbon (rBC). The mass spectra of organics consisted mostly of hydrocarbon fragments (54–86% of total organics), the pattern of hydrocarbon fragments being rather similar regardless of the bus type. Regarding oxygenated organic fragments, ethanol-fueled buses had unique mass-to-charge ratios (m/z) of 45, 73, 87, and 89 (mass fragments of $C_2H_5O^+$, $C_3H_5O_2^+$, $C_4H_7O_2^+$, and $C_4H_9O_2^+$, respectively) that were not detected for the other bus types at the same level. For rBC, there was a small difference in the ratio of C_4^+ and C_5^+ to C_3^+ for different bus types but also for the individual buses of the same type. In addition to organics and rBC, the presence of trace metals in the bus emission particles was investigated.

ARTICLE HISTORY
Received 1 July 2016
Accepted 6 November 2016

EDITOR
Matti Maricq

1. Introduction

A major fraction of particles in urban areas is emitted by traffic, especially diesel vehicles. Particles from diesel engines are mainly composed of soot and a large variety of different organic species. Soot is formed in insufficient burning conditions in the engine (lack of combustion air, poor mixing of air and combustion gases and low combustion temperature) in which hydrocarbon fragments have a greater chance of colliding with other hydrocarbon fragments and growing rather than being oxidized to CO, H_2, CO_2, and H_2O (Bockhorn 1994; Kittelson 1998). Semivolatile organic compounds can condense on soot particles in the exhaust. Organic compounds in engine emissions originate mostly from unburnt (or incompletely burnt) fuel and lubricating oil. It has been suggested that lubricating oil can dominate primary organic aerosol mass loading under typical operating conditions of an engine (Dallmann et al. 2014) but as lubricating oil is composed of cycloalkanes and aromatic compounds it can also be important to the secondary organic aerosol (SOA) formation (Lim and Ziemann 2009).

Besides organic compounds and soot, engine emission particles contain trace elements. In fuel, trace elements can originate from the raw product, like Ni and V in petroleum-based fuel or P in biodiesel, or they may be added during the production and storage of fuel, such as Cu, Fe, Ni, and Zn in petroleum-based fuel and ethanol or Na and K in biodiesel (Korn et al. 2007). Trace elements can also be used as additives in lubricating oil (Rönkkö et al. 2013; Dallmann et al. 2014; Pirjola et al. 2015). Traditionally, the concentrations of trace metals in exhaust particles have been determined by offline methods, but as offline methods need typically rather long sampling periods, the investigation of transient driving cycles is difficult. The Soot Particle Aerosol Mass Spectrometer (SP-AMS) was originally designed to measure submicron refractory black carbon (rBC; also

CONTACT S. Saarikoski sanna.saarikoski@fmi.fi Air Quality, Finnish Meteorological Institute, P.O. Box 503, Helsinki FI-00101, Finland.
*Current affiliation: Institute of Agrarian Sciences, Federal University of Uberlandia, Uberlandia, Brazil.
Color versions of one or more of the figures in the article can be found online at www.tandfonline.com/uast.
Supplemental data for this article can be accessed on the publisher's website.

referred as soot) in particles (Onasch et al. 2012). Since the SP-AMS uses a laser to vaporize chemical species it can also detect some other refractory components, like metals and elements, internally mixed with the rBC particles (Carbone et al. 2015) or as separate particles (Nilsson et al. 2013). The SP-AMS has been proved to be efficient tool in engine exhaust measurements due to its ability to measure refractory material with high time-resolution, (Cross et al. 2012; Carbone et al. 2015) even though the quantification of metals has been shown to be challenging (Carbone et al. 2015; Nilsson et al. 2015).

This article characterizes the chemical composition of exhaust particles from 23 individual city buses in Helsinki, Finland. City buses constitute a significant sector in many public transport systems. In general, the emissions from combustion engines depend on several factors such as engine type, exhaust after-treatment technology, fuel and lubricating oil properties as well as driving and environmental conditions (Maricq et al. 2002; Kittelson et al. 2008; Lähde et al. 2009). Previously city buses were mostly fueled with fossil diesel but in recent years, the utilization of alternative fuels such as biodiesel, ethanol, compressed natural gas (CNG), and hybrid diesel-electric has been increasing in order to decrease emissions and increase the use of renewable energy sources.

In addition to alternative fuels, the emissions from the buses have been reduced by developing engine technologies and by using exhaust after-treatment systems (ATSs). ATSs typically decrease solid particle number and mass concentrations but they can also change the chemical composition of emission particles as their functioning depends on the chemical species in question. For instance, oxidative exhaust after-treatment like diesel oxidation catalyst (DOC) and diesel particulate filter (DPF) with catalytic coating can increase particulate phase sulfur (Maricq et al. 2002; Arnold et al. 2012; Rönkkö et al. 2013). On the other hand, DOC and selective catalytic reduction (SCR) decreased the concentration of organics in heavy-duty diesel engine particles whereas the soot concentration remained nearly at the same level (Karjalainen et al. 2012). A substantial reduction of soot can be obtained by using a DPF (Robinson et al. 2015) but some engine technologies like the exhaust gas recirculation (EGR; Gomaa et al. 2010) can increase the emission of soot. Engine and exhaust after-treatment technology choices can also alter the physical and chemical properties of organics and soot. For example the use of the DOC has been observed to result in more oxidized organics in particles (Chirico et al. 2010) whereas the morphology and structure of soot, and therefore also its reactivity, may alter by the use of the EGR (Al-Qurashi and Boehman 2008; Li et al. 2015). In terms of metals, ATSs can even be the source of selected metals (Johnson 2013). Besides primary particulate material and particulate material formed during the immediate dilution and cooling of the exhaust, the application of ATS can also have an impact on the formation of SOA from the engine emissions. The presence of DOC and DPF has been shown clearly reduce the SOA production (Chirico et al. 2010).

The buses investigated in this study operated with different engines, ATSs, and were fueled by diesel, diesel-electric, ethanol, and CNG. Buses represented EURO III, EURO IV and EEV (Enhanced Environmentally Friendly Vehicle) emission levels (see details in https://www.dieselnet.com/standards/eu/hd.php). As the same ATS and fuel combination can be used to achieve different emission levels, this study classifies investigated buses mainly based on their emission levels and fuels, not the exhaust after-treatment techniques applied. Regarding the bus fleet in Helsinki in 2013, when this study was conducted, the fleet consisted mostly of EEV (>60%) and EURO III (~20%) level buses whereas EURO II, EURO IV, EURO V, and EURO VI level buses constituted <5% of the buses individually (HSL Helsingin seudun liikenne ympäristöraportti 2014, see https://www.hsl.fi/sites/default/files/uploads/hsl_ymparistoraportti_2014.pdf). In terms of alternative fuels, the fraction of CNG buses in Helsinki fleet was <3% in 2013 while only a few ethanol and hybrid buses operated in Helsinki in 2013. In the future, the majority of Helsinki area bus fleet is, however, supposed to be composed of EURO VI level buses together with the total electric buses. Also fossil diesel fuel will be replaced completely by biodiesel.

In this study, the bus emissions were measured by chasing the buses with a mobile laboratory van at two locations; at a bus depot area and on the normal route of bus line 24. At the depot, the purpose of the measurements was to compare several different buses in controlled driving conditions whereas the aim of the on-road measurements was to examine few buses in their real driving conditions. This is the second article presenting the results from the bus emission measurements. In the first article of Pirjola et al. (2016), the focus was on particle number concentrations and size distributions together with emission factors for major gas and particulate phase pollutants. Chemical composition of particles was discussed in the first article only briefly. The objective of this article was to investigate the detailed carbonaceous composition of the bus emission particles for several engine/fuel/ATS combinations as well as the presence of trace metals in particles. In the previous article by Pirjola et al. (2016), it was shown that the emitted particle mass concentrations varied greatly depending on the bus type. The aim of this article is to elucidate to

what extent this variation can be seen in particle chemical composition. In addition, this article discusses the performance and features of the SP-AMS to detect refractory material in emission particles.

2. Experimental

2.1. Measurement design

The measurement scheme is presented in detail in Pirjola et al. (2016) and therefore only a short description is given here. The exhaust emissions of individual city buses were studied by using a mobile laboratory van "Sniffer" (VW LT35 diesel van; Pirjola et al. 2004). Emissions from 23 individual buses were measured including EURO III, EURO IV, and EEV class buses with different after-treatment system, fuel, and engine (Table 1). ATSs comprised DPF, SCR, and three-way catalyst (TWC). Additionally, EURO IV and EEV-EGR-DPF buses had a EGR to reduce NO_x emissions. Buses were fueled with fossil diesel, ethanol, and CNG fuel and they had three different types of lubricating oil (type 1: EURO III, EEV-SCR and hybrid buses, type 2: EURO IV, EEV-EGR-DPF, and CNG buses, type 3: ethanol buses) but unfortunately the exact type and composition of lubricating oils could not be tracked even though it was known that all lubricating oils were obtained from the same manufacturer (Teboil).

At the bus depot, the buses were driving a 0.5 km circle, which consisted of two stopping points, two accelerations, two decelerations, and a constant speed period (Figure S1). This circle was repeated ten times for each bus. Sniffer was chasing the examined bus at around 5 m distance. Some of the buses arrived from their normal route for the depot tests, and were sufficiently warm already whereas the others were warmed-up by idling for 30 min before the measurements. Specific information which buses used idling is not available. Regarding the engine temperatures (Table S1), they varied rather largely between the buses and especially the engine temperatures for the EURO III buses were rather low.

In addition to the bus depot, Sniffer was chasing buses on their normal route (line 24) in southwestern Helsinki in two consecutive evenings (Figure S1). Six individual buses were measured on line 24 and they presented four different bus types (EURO III, hybrid, ethanol, and CNG; Table 1). One hybrid and one CNG bus was measured on both evenings. Ethanol and both hybrid buses were the same individuals that were also measured at the bus depot. Regarding the meteorological conditions during the measurements, the average wind speed was 2.7 ± 1.6 m s^{-1}, the temperature varied from 5.3°C to 7.9°C and the relative humidity was in the range of 72–81%.

2.2. Soot particle aerosol mass spectrometer

The chemical composition of PM_1 particles was measured by using a SP-AMS (Aerodyne Research

Table 1. Technical information of the buses investigated at the bus depot and line 24.

Bus no	Year	Engine[1]	Mileage (10^3 km)	EU standard	ATS[2]	Fuel[3]	Testing location
273	2002	SCANIA	750	EURO III	no	Diesel	Depot
425	2004	SCANIA	900	EURO III	no	Diesel	Depot
429	2004	SCANIA	1150	EURO III	no	Diesel	Line 24
501	2005	SCANIA	890	EURO III	no	Diesel	Depot
614	2006	SCANIA	835	EURO IV	EGR+DPF	Diesel	Depot
617	2006	SCANIA	790	EURO IV	EGR+DPF	Diesel	Depot
618	2006	SCANIA	700	EURO IV	EGR+DPF	Diesel	Depot
810	2008	VOLVO	620	EEV	SCR	Diesel	Depot
945	2009	VOLVO	400	EEV	SCR	Diesel	Depot
946	2009	VOLVO	390	EEV	SCR	Diesel	Depot
821	2008	SCANIA	575	EEV	EGR+DPF	Diesel	Depot
1006	2010	SCANIA	530	EEV	EGR+DPF	Diesel	Depot
1007	2010	SCANIA	525	EEV	EGR+DPF	Diesel	Depot
1129	2012	SCANIA	280	EEV	EGR+DPF	Diesel	Depot
1201	2012	VOLVO-HYB	135	EEV	SCR	Diesel-electric	Depot and Line 24
1202	2012	VOLVO-HYB	130	EEV	SCR	Diesel-electric	Depot and Line 24
1342	2013	SCANIA-ETH	5	EEV	TWC	RED95	Depot
1343	2013	SCANIA-ETH	5	EEV	TWC	RED95	Depot and Line 24
709	2007	MAN-CNG	685	EEV	TWC	CNG	Line 24
731	2006	MAN-CNG	650	EEV	TWC	CNG	Depot
732	2006	MAN-CNG	680	EEV	TWC	CNG	Line 24
734	2006	MAN-CNG	555	EEV	TWC	CNG	Depot
736	2006	MAN-CNG	500	EEV	TWC	CNG	Depot

[1]CNG buses had spark-ignition engines, all other engines were compression ignited.
[2]After-treatment system.
[3]Diesel fuel included 7% renewable diesel (NEXBTL), Hybrid buses (diesel-electric) recharged their batteries during braking, ethanol fuel (RED95) contained 95% ethanol, 5% water, and additives, and CNG contained 98% of methane and 2% of both ethane and nitrogen as well as trace amounts of propane, carbon dioxide and oxygen but no sulfur or heavy metals.

Inc., USA). The operation of the SP-AMS is presented in Onasch et al. (2012) and given here briefly. In the SP-AMS, an intracavity Nd:YAG (neodymiumdoped yttrium aluminum garnet) laser vaporizer (1064 nm), based on the design of the single particle soot photometer (SP2; Droplet Measurement Technologies, Boulder, CO, USA), is incorporated into the Aerodyne High Resolution Time-of-Flight Aerosol Mass Spectrometer (HR-ToF-AMS; Aerodyne Research Inc., Billerica, MA, USA). The SP-AMS enables the measurement of rBC in addition to the non-refractory species determined with the standard AMS using a tungsten vaporizer at 600°C (sulfate, nitrate, ammonium, chloride, and organics). The SP-AMS can operate in two modes, mass spectra (MS) mode, in which the average chemical composition is measured over the size range of the instrument (~40–1000 nm), and particle-Time-of-Flight mode, in which the chemical species are determined as a function of the particle size. In the MS mode, the chopper is alternated between open and closed positions of which open allows the particle beam to pass through and closed blocks it. Closed position is used to determine the instrumental background, including gas-phase species, which is subtracted from the signal achieved when the chopper is in open position. In this study the SP-AMS measured only in the MS mode as the data was recorded in 5 s time-resolution (2.5 s open and 2.5 s closed) in order to capture the different stages of the driving cycle (acceleration, deceleration, and steady driving). Both laser and tungsten vaporizers were installed (and used) during the measurements. In addition to the SP-AMS, black carbon was also measured by an Aethalometer (Ambient Air Quality Monitoring AE 33, Magee Scientific, Berkeley, CA, USA). In this article BC concentrations from the aethalometer were utilized only for the comparison with the SP-AMS rBC data (see next section).

2.3. Data analysis

The default collection efficiency (CE) of 0.5 (Canagaratna et al. 2007) was used for the SP-AMS data as CE could not be explicitly determined due to the lack of applicable collocated measurements. Regarding rBC a default relative ionization efficiency (RIE) of 0.2 was used for rBC (Onasch et al. 2012). However, compared to the aethalometer, rBC from the SP-AMS was significantly smaller than BC from the aethalometer. Although the measurements in the SP-AMS and aethalometer are based on different techniques, the reason for the lower rBC concentrations measured by the SP-AMS was assumed to be systematical and due to the imperfect laser-to-particle beam alignment. Therefore, rBC from the SP-AMS data was corrected by multiplying it by the ratio of BC to rBC calculated separately for each bus type. The ratio of BC to rBC varied from 1.2 (EURO IV) to 5.0 (ethanol).

For the metals detected in the particles (V, Cr, Al, P, Mn, Ni, K, Sr, Cd, Cu, Fe, Zn, Na, Ba, and Zr) the signal given by the SP-AMS was converted to the mass concentration by using the RIEs given in Carbone et al. (2015). If the exact RIE was not available (P, Zr, K, and Cd) a default value of 1 was used. Although P is nonmetallic, it is discussed together with the metals hereafter. More detailed description of the calculation of the mass concentrations from the SP-AMS is given in the online supplementary information (SI). Additionally, the factors affecting the CE and RIE in the SP-AMS are discussed in the SI.

For the data collected at the bus depot, only the average concentrations over the whole route (10 circles) are presented. However, the variability within the test circles is given in Table S2 for the metals and in Figure S2 for organics and rBC (by standard deviations). The variability in the emission measurements of individual buses is discussed in general in the SI. Bus-type averages (with standard deviations) were calculated by averaging the results obtained for the individual buses of the same bus type (2–4 depending on the bus type). For the buses driving on line 24, only the averages over the whole route were calculated.

All the results presented here have been subtracted by the background concentrations if not stated otherwise. Background measurements for the bus depot were performed at the depot when there were no buses driving nearby and on-road by standing at the location where there was no direct impact from traffic. The contribution of background to the total measured concentrations for chemical species is given in Table S3. For organics the contribution of background was largest for the hybrid and ethanol buses being equal to 40–50% and ~60% at the bus depot and on-road measurements, respectively. For rBC, the contribution of background to the total measured rBC concentrations was <25% for all the bus types whereas for inorganic species (sulfate, nitrate, ammonium, and chloride) the measured concentrations were largely due to the background concentrations. In case of metals, for Al, Ba, Cr, P, Na, Sr, and Cd their concentrations in the bus emission particles were smaller than their concentrations in background particles for most of the bus types (Table S3). On the other hand, for Zn, Fe, Cu, and K the contribution of background was moderate for most of the buses.

2.4. Physical characterization of bus emission particles

The instrumentation for the physical characterization of particles (and the monitoring of gases) deployed in Sniffer is described in Pirjola et al. (2016). Particle number concentrations and size distributions were measured with an Engine exhaust particle sizer (EEPS, model 3090, TSI Inc., Shoreview, MN, USA), two electrical low pressure impactors (ELPI, Dekati Ltd., Tempere, Finland) and an ultrafine condensation particle counter (CPC model 3776, TSI Inc.). Regarding the observed number size distributions, there were differences in the size distributions between the bus types even though bimodal shapes were measured for all the buses (Pirjola et al. 2016). EURO III, ethanol, hybrid, and EEV-SCR buses had a pronounced mode at ~10 nm compared to that of the soot mode peaking typically at ~60–80 nm. The physical characteristic of exhaust particles are not discussed further in this article as they were already presented in Pirjola et al. (2016) and the focus of this article is on the chemical species measured by the SP-AMS.

3. Results and discussion

Bus emission particles (PM_1) were dominated by organics and rBC regardless of the bus type measured (Figure 1a). It was clear that the newer standard diesel-fueled buses with the exhaust after-treatment systems (EURO IV and EEV level buses) emitted less organics than the older ones without any ATS (EURO III level buses). For rBC, the trend was similar to organics except for the EURO IV buses that had almost similar level of rBC than the EURO III buses. Of alternative fueled buses, ethanol buses had very small emissions of both rBC and organics whereas the CNG buses emitted organics similar level with the EEV-buses. For most of the buses, the fraction of organics was larger than that of rBC varying from 34% of mass (hybrid) to 99% of mass (CNG), on average. For all the bus types the concentrations of rBC and organics were higher during acceleration than steady driving; however, the mass fraction of rBC was larger during acceleration than steady driving for the ethanol and CNG buses (Pirjola et al. 2016). In addition to organics and rBC, a small fraction of PM_1 was composed of inorganic species (nitrate sulfate, ammonium, and chloride; Figure 1a).

3.1. The composition of particulate organics

The mass spectra of organics was dominated by hydrocarbon fragments ($C_xH_y^+$; Figure 2). The largest fraction of hydrocarbons was measured for the EURO III (86%) and CNG (80%) buses and the smallest for the hybrid (54%), ethanol (55%) and EEV-EGR-DPF buses (56%; Figure 1a). Besides hydrocarbons organics consisted of the fragments with one oxygen atom ($C_xH_yO^+$) or several oxygen atoms ($C_xH_yO_z^{+,\ z>1}$). The contributions of hydrocarbons and oxygenated fragments were similar during acceleration and steady driving for the EURO III and ethanol buses whereas for all the other bus types hydrocarbon fraction was larger during acceleration than in constant driving. The elemental ratios for organics are given in Pirjola et al. (2016). In line with the fractions of hydrocarbon and oxygenated organic fragments presented in this article, the largest hydrogen to carbon ratio (H:C) and smallest oxygen to carbon (O:C) ratio was measured for the CNG and EURO III buses and the smallest H:C and largest O:C was measured for the hybrid, EEV-EGR-DPF and ethanol buses.

The pattern of hydrocarbon fragments was relatively similar for all the bus types (Figure 2). There were some differences in the pair of alkene ($C_xH_{2x-1}^+$) and alkane ($C_xH_{2x+1}^+$) type of fragments, for example, $C_3H_5^+$ (mass-to-charge ratio (m/z) 41) and $C_3H_7^+$ (m/z 43), $C_4H_7^+$ (m/z 55) and $C_4H_9^+$ (m/z 57), and $C_5H_9^+$ (m/z 69) and $C_5H_{11}^+$ (m/z 71) for the measured bus types. Since diesel fuel and lubricating oil are processed with different techniques, their organic MS can be unlike. It has been suggested that lubricating oil MS is enriched in cycloalkanes whereas diesel fuel MS has more n-alkanes and branched alkanes resulting in larger ratio of alkene to alkane fragments for lubricating oil than diesel fuel (Tobias et al. 2001). As an example, the correlation between $C_4H_7^+$ and $C_4H_9^+$ for each bus type is given in the SI (Figure S3). For the EURO III and EEV-SCR buses the ratio of $C_4H_7^+$ to $C_4H_9^+$ resembled that of lubricating oil whereas for the EURO IV and EEV-EGR-DPF buses the ratio was smaller being closer to that of diesel fuel.

For oxygenated organic fragments the dominant fragment in the $C_xH_yO_z^{+,\ z>1}$ group was CO_2^+ (m/z 44) while $C_xH_yO^+$ group consisted mostly of CO^+ (m/z 28) and CHO^+ (m/z 29) fragments. However, the mass spectra for the ethanol buses differed from those for the other bus types in terms of oxygenated organic fragments. The largest signal in the $C_xH_yO^+$ group for the ethanol buses was $C_2H_5O^+$ at m/z 45 (Figure 2). In addition to the $C_2H_5O^+$ fragment, the MS for the ethanol buses had distinctive signals at m/z 73, 87 and 89 corresponding to $C_3H_5O_2^+$, $C_4H_7O_2^+$, and $C_4H_9O_2^+$ fragments, respectively. The concentrations of oxygenated fragments were largest when the ethanol buses accelerated at the bus depot the fraction of $C_2H_5O^+$ in total organics being ~5% whereas the corresponding fractions of the other oxygenated fragments were <1% individually

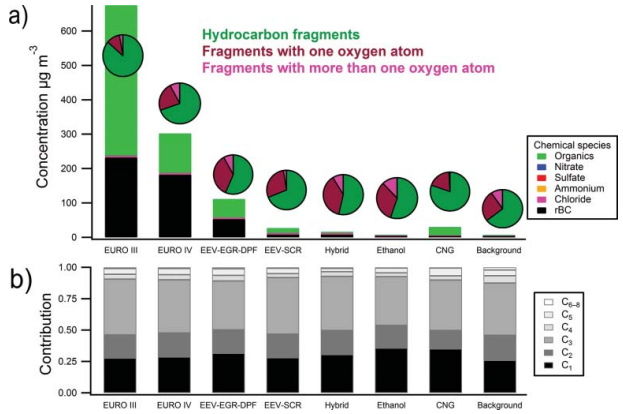

Figure 1. Average chemical composition of PM_1 particles for each bus type and background measured at the bus depot. Major chemical species (bars) and the composition of organics (pies) (a), and the C_x fragments of rBC (b). Background concentrations have been subtracted from the bus-type concentrations.

(Figure S4). In addition to the bus depot, the oxygenated fragments were also present in the MS measured for the ethanol bus in on-road measurements (Figure S5). However, their fractions in organics were smaller on-road than at the depot and especially the fractions of $C_3H_5O_2^+$ and $C_4H_7O_2^+$ were at similar level on-road and at the background (Figure S4). $C_2H_5O^+$, $C_3H_5O_2^+$, $C_4H_7O_2^+$, and $C_4H_9O_2^+$ fragments were also detected for the other bus types but their fraction in organics was much smaller than for the ethanol buses (Figure S6).

The origin of oxygenated fragments detected for the ethanol buses was not clear. $C_2H_5O^+$ fragment can be speculated to originate from gas-phase ethanol (C_2H_5OH) that condenses onto the particles when the exhaust was diluted in ambient air and its temperature decreased. Ethanol is, however, quite volatile thus its presence in the particle phase is somewhat doubtful. It is

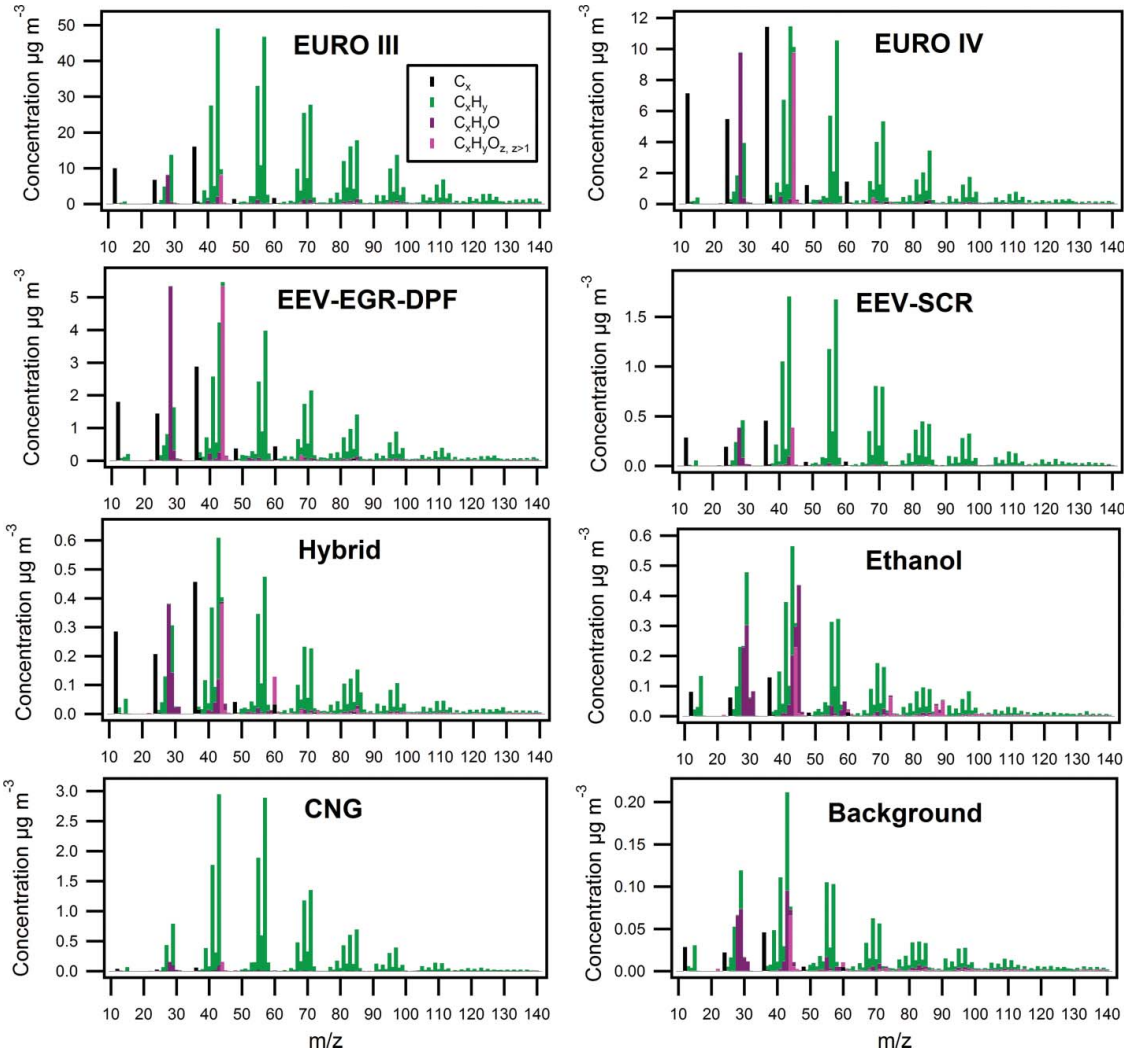

Figure 2. Average mass spectra for organics and rBC for each bus type measured at the bus depot. MS measured at the background location are presented separately and were not subtracted from the bus emission MS.

also possible that oxygenated fragments are derived from additives used in ethanol fuel or lubricating oil as the ethanol buses had different lubricating oil from the other bus types. For example in the study of Yu et al. (2012) they attributed the strong signals at m/z 85 and 113 (specifically the $C_6H_9O^+$ and $C_8H_{13}O^+$ fragments) to synthetic esters used in aircraft lubricating oil. Moreover, it cannot be excluded that oxygenated fragments were formed in the after-treatment system (TWC; Table 1) used in the ethanol buses.

For the hybrid buses there was a large signal for the oxygenated fragment $C_2H_4O_2^+$ at m/z 60 (Figure 2). The concentration of $C_2H_4O_2^+$ was almost ten times larger and its fraction in organics nearly 30 times greater for the hybrid buses than for the other bus types at the bus depot on average (Figure S6). $C_2H_4O_2^+$ fragment is typically associated with biomass burning aerosol (Aiken et al. 2009); however, it has a contribution of ~0.3% to total organics in urban areas in the absence of biomass burning influence. In this study, the contribution of $C_2H_4O_2^+$ to the background organics was ~0.4 and ~0.9% measured at the depot and on-road, respectively (Figure S7), the larger contribution on-road probably due to the larger impact of wood burning during the on-road measurements. Typically, the contribution of wood burning to the concentrations of organic matter is ~10–20% in autumn in Helsinki depending on weather conditions (e.g., temperature, wind direction, and speed; Saarikoski et al. 2008; Saarnio et al. 2012). The origin of $C_2H_4O_2^+$ fragment in the hybrid bus emissions remained unclear. Hybrid buses used the same lubricating oil with the EURO III and EEV-SCR buses but for those buses the contribution of $C_2H_4O_2^+$ was very small. Hybrid buses were equipped with a SCR but it was also in the EEV-SCR buses. As discussed earlier in Pirjola et al. (2016) hybrid buses also differed from the other bus types as they emitted larger concentrations of ammonium, especially during on-road measurements, that was probably related to the SCR (Figure S8).

The average MS of organics measured for each bus type (Figure 2) was compared with the reference MS for diesel bus, diesel truck, diesel generator, diesel fuel and lubricating oil (Table S4). Reference MS were obtained from the AMS spectral database (http://cires1.colorado.edu/jimenez-group/AMSsd). All the diesel-fueled buses investigated in this study (EURO III, EURO IV, EEV-EGR-DPF, EEV-SCR, and hybrid) had similar MS with the reference MS for a diesel bus (Canagaratna et al. 2004) and diesel truck (Mohr et al. 2009) but none of the MS correlated clearly with the reference MS for the diesel generator (Sage et al. 2007). Compared to the reference MS of unburnt diesel fuel and lubricating oil (Canagaratna et al. 2004) diesel-fueled buses had more similar MS to the reference MS of diesel fuel than to those of lubricating oil, however, the fraction of m/z 57 was larger in the MS of diesel fuel than in the MS of bus emissions (Figure S9). In the reference MS of lubricating oil especially the fractions of m/z 43 and 57 were significantly smaller than in the MS of bus emissions in line with the larger ratio of alkene to alkanes for lubricating oil as discussed earlier. As expected the MS of the ethanol buses did not resembled that of the diesel-fueled vehicles, or lubricating oil, but the MS of the CNG buses was very similar to that of diesel bus, diesel truck and diesel fuel.

The MS of organics for the bus emission particles were also compared with the reference MS of hydrocarbon-like organic aerosol (HOA) detected in ambient air (Table S4). Excluding the MS for the ethanol buses, the MS of bus emissions reminded of those of ambient HOA. The correlation between bus emission MS and HOA MS was strongest for HOA measured near a highway in Helsinki, Finland (Aurela et al. 2015); however, the fractions of m/z 43 and 57 were larger for bus emissions than for HOA, especially for the CNG buses (Figure S9). The MS of bus emissions were also compared with HOA calculated by using multiple datasets (Ng et al. 2011; Crippa et al. 2014) the correlation coefficients being slightly larger with HOA from Ng et al. (2011) than from Crippa et al. (2014). The MS were compared in unit mass resolution (UMR) based so the high resolution (HR) data was converted to UMR by summing up all the HR ions detected at the same nominal m/z.

3.2. Refractory black carbon

Refractory BC was composed of carbon fragments from C_1^+ to C_9^+ the largest signal obtained for C_3^+ followed by C_1^+ and C_2^+ (Figure 1b). The C_x pattern was similar for acceleration and steady driving (Figure 3a) and also regarding different bus types, the general trend of carbon fragments was rather comparable (Figure 2). Additionally, individual buses of the same type emitted similar C_x patterns, except the EEV-EGR-DPF buses. Four individual EEV-EGR-DPF buses were investigated at the depot (Table 1) of which two buses emitted larger concentrations of organics than the other two (Figure S2). These larger emitters (buses no 1006 and 821; called hereafter "dirty EEV-EGR-DPF") had higher concentrations of C_5^+, C_1^+, and C_4^+ compared to the concentration of C_3^+ whereas the remaining two buses (buses no 1007 and 1129 called hereafter "clean EEV-EGR-DPF") emitted significantly smaller concentrations of C_5^+, C_1^+, and C_4^+ compared to that of C_3^+. It is known that a fraction of the C_1^+ signal detected by the SP-AMS can be present also

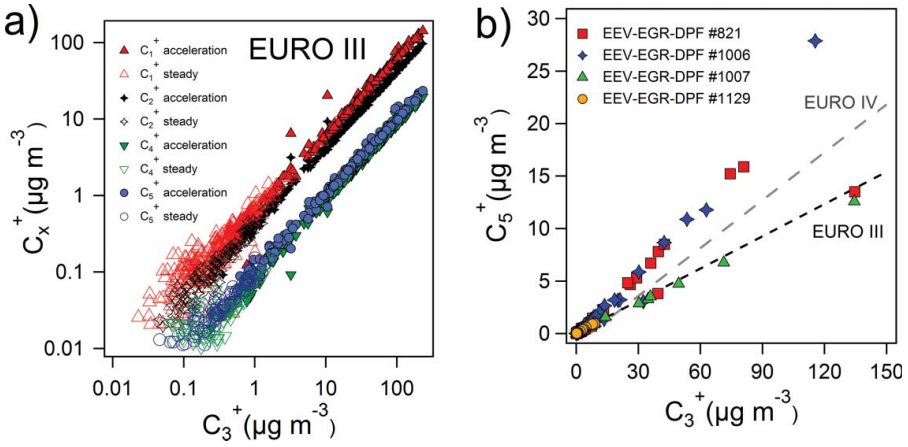

Figure 3. Refractory black carbon fragments. C_3^+ versus C_1^+, C_2^+, C_4^+, and C_5^+ for the EURO III buses during acceleration and steady driving (a) and C_3^+ versus C_5^+ for the individual EEV-EGR-DPF buses and the average for the EURO III and EURO IV buses (b).

with the laser off, that is, originate from organic compounds, but for C_2^+ and greater carbon fragments there is signal only with the laser on (Onasch et al. 2012). For the "clean EEV-EGR-DPF" buses, the ratio of C_5^+ to C_3^+ was similar to the average of the EURO III buses; however, for the "dirty EEV-EGR-DPF" buses that ratio was even greater than the average for the EURO IV buses (Figure 3b). Of these buses bus no 1129 had clearly lower rBC concentration but for the other three buses the concentrations of rBC were quite similar (Figure S2).

As there were no clear differences in the driving pattern of individual EEV-EGR-DPF buses, the discrepancy in the rBC fragments was expected to be related to the soot formation in the engine, possibly affected by the EGR, or the functioning of the exhaust after-treatment system (DPF). EGR is an effective technique to reduce NOx emission from diesel engines but the use of EGR can increase soot emissions (Gomaa et al. 2010). Therefore in EGR-equipped vehicles soot is typically collected into the DPF where it is oxidized in regeneration process mainly to CO_2. Regarding the buses investigated in this study, also the EURO IV buses had EGR and DPF (Table 1). Since also the EURO IV buses had a slightly elevated fraction of C_1^+, C_4^+, and C_5^+ in rBC (and larger ratio of C_5^+ to C_3+ than, for example, EURO IIII; Figure 3b) C_x fragmentation pattern observed for the "dirty EEV-EGR-DPF" and EURO IV buses is likely to be related to the transformation of soot by the influence of EGR or DPF. It has been shown earlier that the EGR can change surface, nanostructure, and oxidative properties of soot (Al-Qurashi and Boehman 2008; Li et al. 2015).

The composition of organics was also slightly different for the two EEV-EGR-DPF types; the "dirty EEV-EGR-DPF" buses had clearly larger fraction of $C_xH_yO_{z,\ z>1}^+$ (mostly CO_2^+) and therefore also greater O:C and smaller H:C than those for the "clean EEV-EGR-DPF" buses. CO_2^+ fragment is typically associated with highly oxidized organics (Aiken et al. 2009) but in this case it could be refractory CO_2^+ (rCO_2^+) as it increased together with some carbon fragments (C_1^+, C_4^+ and C_5^+). The origin of rCO_2^+ is uncertain; however, Corbin et al. (2014) speculated it to be due to (i) oxygenated functional groups incorporated into the refractory structure of rBC, (ii) fragmentation of refractory organic material, (iii) CO or CO_2 adsorbed to the particle surface, (iv) gaseous CO or CO_2 trapped within internal voids, or (v) reaction of carbon vapor with gas-phase O_2.

3.3. Trace metals

V, Cr, Al, P, Mn, Ni, K, Sr, Cd, Cu, Fe, Zn, Na, Ba, and Zr were detected in the bus exhaust particles. Of these metals, the largest concentrations were found for K, followed by Zn, Na, Fe, and P. Regarding different bus types, the concentrations of metals followed mostly the pattern of organic and rBC concentrations the largest concentrations detected for the EURO III buses followed by the EURO IV and EEV-EGR-DPF buses (Figure S10). Zn and P deviated from the majority of the metals as the particles emitted from the EEV-EGR-DPF buses had larger concentrations of Zn and P than particles from the EURO IV buses. However, for all the bus types the ratio of P to Zn was rather similar (Figure 4). Zn and P have been earlier associated with lubricating oil (Rönkkö et al. 2013; Dallmann et al. 2014; Pirjola et al. 2015) and, besides as oil additives, metals can be present in lubricating oil due to engine wear or contamination, (e.g., Fe and Cu; Yawar 2010). Also diesel fuel can contain some metals, for example, Zn, Cr, Mo, Ti, Cu, Ni, Co, Ba, Mn,

and V, even though the largest metal concentrations in diesel fuel have been measured for "crustal-type species" like Si, Ca, Al, Fe, and Mg (Wang et al. 2003). Metals may also originate from the ATSs used in the buses (Johnson 2013).

Ethanol buses emitted the largest concentration of Cu and also elevated concentrations of Fe; however, the difference between the two individual ethanol buses was significant shown by the large standard deviations for Cu and Fe (Figure S10). Elevated trace metal concentrations for the ethanol vehicles have been associated with ethanol fuel production, storage, and transportation (Bruning and Malm 1982). The presence of trace metals in ethanol fuel has an influence on the engine maintenance as the metallic species can accelerate the corrosion of engine or promote the formation of, for example, sediments (Taylor and Synovec 1993).

Most of the metals correlated with the concentration of rBC; however, the relationship between the metals and rBC was different for acceleration and steady driving (Figure S11). For example, the ratio of V to rBC decreased as rBC increased for steady driving whereas during acceleration V/rBC remained nearly the same regardless of the rBC concentrations (Figure S11b). This may suggest that in steady driving rBC and V had different origin whereas during acceleration they were associated with the same source. That trend was observed for all the metals for the EURO III and EEV-EGR-DPF buses whereas for the EURO IV buses Zn and P displayed different behavior. For the EURO IV buses there were similar slopes for Zn/rBC to rBC for acceleration and steady driving indicating that Zn and rBC were not emitted with the same ratio (from the same source) either during acceleration or constant driving (Figure S11d). P followed similar trend with Zn for the EURO IV buses.

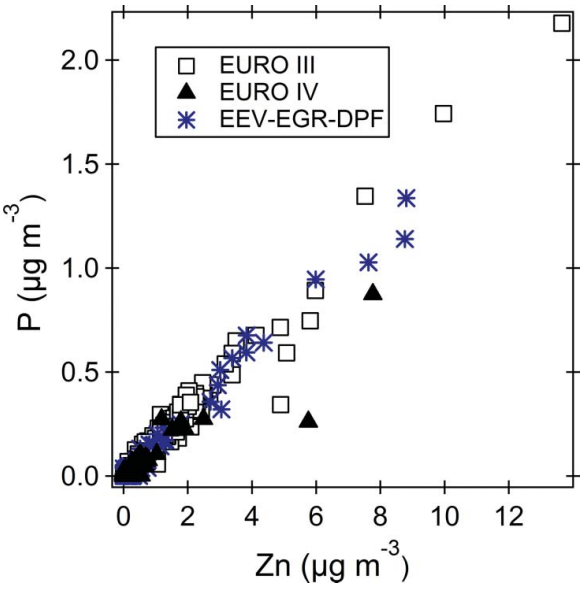

Figure 4. Correlation of Zn and P for the EURO III, EURO IV, and EEV-EGR-DPF buses.

There can be several reasons for the different behavior of metals with rBC. In addition to the different sources in the engine and/or ATS, also the detection efficiency of the SP-AMS depends on the mixing state of metals and rBC as well as their concentrations in the sample. In the SP-AMS, metals can be vaporized either in the laser beam or at tungsten vaporizer if they are both installed. The metals associated with the rBC particles are vaporized with the laser (Carbone et al. 2015); however, the detection efficiency for the metals can depend on the concentration ratio of metal to rBC. By comparing the SP-AMS with the ICP-MS it has been shown that the two techniques agreed better for the metals when the concentrations of rBC were high the disagreement being greater for the periods of low rBC (Carbone et al. 2015).

If the metals are vaporized at the tungsten vaporizer, slow evaporation can be an issue regarding the quantification of the metals (Salcedo et al. 2012). In slow evaporation, chemical species evaporate from the tungsten vaporizer on slower time scale than the nonrefractory material. As a result, chopper open and closed signals become a combination of the particle signal entering the instrument and the signal of residual components slowly evaporating from the vaporizer. In this study, the elevated ratio of closed to open signal was observed for Zn, Cu, Na, and K (Table S5) indicating that at least a fraction of those species was in the particles with no rBC. P had no evidence on slow evaporation (Table S5); however, that does not exclude P as being externally mixed with rBC as P has a low evaporating temperature (280°C) that allows its fast evaporation at tungsten vaporizer at ~600°C.

3.4. On-road measurements for bus line 24

In addition to the controlled tests at the bus depot, the emissions from the buses were investigated on-road in their normal driving route. Six buses were measured on line 24 presenting four different bus types; EURO III, hybrid, ethanol, and CNG. Regarding organics and rBC the concentrations at the depot and on-road were rather similar for hybrid, ethanol, and CNG buses whereas for the EURO III buses organic and rBC concentrations were seven and four times larger at the depot than on-road, respectively (Figure 5). The reason for the larger concentrations at the depot can be speculated to be due to, for example, the different speed and acceleration rate in the depot and on-road (Pirjola et al. 2016). For individual buses, the difference between the depot and on-road measurements is discussed in the SI.

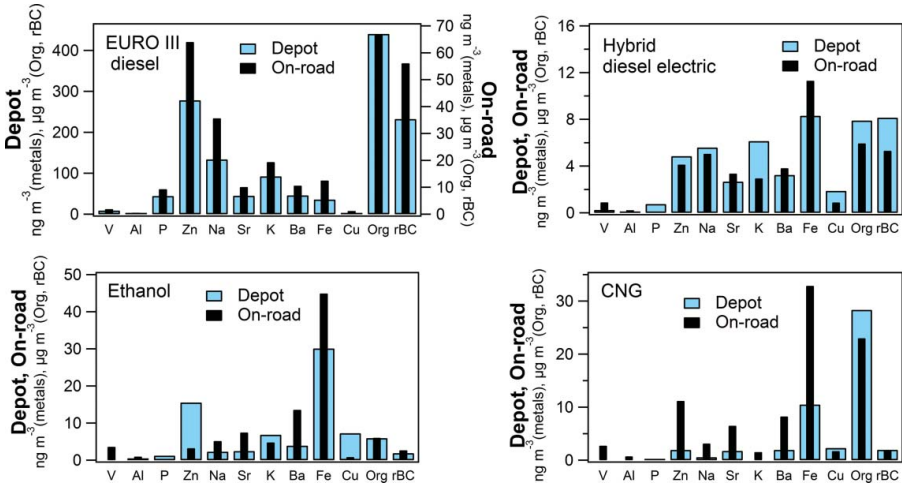

Figure 5. Bus-type average concentrations of V, Al, P, Zn, Na, Sr, K, Ba, Fe, Cu, organics (Org), and rBC for the EURO III, hybrid, ethanol, and CNG buses at the depot and on-road. For K the concentrations are divided by 100 and for Sr and Ba multiplied by 100 in order to get them to the same scale. Note that the EURO III has different *y*-axes for the depot and on-road concentrations.

The pattern of major metals (V, Al, P, Zn, Na, Sr, K, Fe, and Cu) was very similar for the EURO III buses at the depot and on-road (Figure 5), but like the concentrations of organics and rBC, metal concentrations were much smaller in on-road measurements than at the depot (approximately four times smaller concentrations on-road). For the hybrid and ethanol buses, the levels of metals measured at the depot and on-road were more similar than for the EURO III buses but there were slightly larger concentrations of Fe in on-road measurements for both bus types. For the CNG buses, in addition to Fe, also other metals were larger on-road than at the depot. In Pirjola et al. (2016) larger emissions on-road for the CNG buses were suggested to result from different operating conditions at the depot and on-road (e.g., engine load) that could affect the consumption of lubricating oil. Metals, especially Fe, may also originate from other traffic sources than fuel or lubricating oil, for example from brake wear, tyre wear, road surface, or other nonexhaust sources. Whereas in other areas there may be additional background sources of metals, in Helsinki there is no significant industrial activity, and prior measurements have attributed a large fraction of ambient metal concentrations to long-range transport (Pakkanen et al. 2001).

4. Summary and conclusions

This article describes the mass spectral signatures of submicron particles emitted from several different bus types operated with various after-treatment systems and fuels. In general, significant differences in mass concentrations were detected between the bus types, which was anticipated as the emission standards of the measured buses varied from EURO III to EEV. The chemical composition of emission particles changed much less with the bus type. Organic fraction was dominated by hydrocarbon fragments with similar mass spectra not being specific for the bus characteristics. For oxygenated fragments, there were differences between the bus types. Ethanol-fueled buses had specific oxygenated fragments $C_2H_5O^+$, $C_3H_5O_2^+$, $C_4H_7O_2^+$, and $C_4H_9O_2^+$ that were not detected for the other bus types at comparable levels. Hybrid buses emitted larger amount of $C_2H_4O_2^+$ at m/z 60 than the other bus types. $C_2H_4O_2^+$ fragment is typically associated with biomass burning, but as shown in this study, it can also be related to the other combustion sources.

The composition of rBC showed some evidence for being indicative for the soot formation in the engine or the functioning of the after-treatment system. In order the after-treatment technology to be beneficial from the environmental perspective, it needs to be reliable and operate in repeatable manner, but as this study showed, there can be significant differences in the emissions of individual buses of the same type. Also several metals were detected in the bus emission particles. The pattern of metals was not found to be unique either for the fuel or lubricating oil type but the metal patterns observed at the bus depot and on-road measurement followed each other closely, especially for the EURO III buses, confirming that the bus exhaust produced a unique combination of metals.

In this study emission from the buses were investigated by chasing the buses with a mobile laboratory van. That enabled to examine a number of buses in a relatively short time in controlled driving conditions at the bus depot. Even though the driving pattern was similar for all the buses, the weakness of this study was that

warm-up was not necessarily identical for all the buses, which could have affected the emissions. Additionally, the results of this study may not be representative for all the bus types studied as only two to four individual buses of the same type were examined. Furthermore, the interpretation of the results was complicated by the lack of information on the history and operation of individual buses, for example, the type of lubricating oil and the duration from the last oil change was not obtainable. In the future, it would also be beneficial to examine the composition of used fuel and lubricating oil with the SP-AMS. Regarding the bus types, unfortunately EURO VI level buses were not available for the measurements. EURO VI buses together with total electric buses are supposed to constitute majority of Helsinki area bus fleet in the future.

The chemical composition of particles was examined by using the SP-AMS. The advantage of using the SP-AMS in emission studies is its ability to measure rapidly changing concentration and composition of non-refractory and refractory material. For rBC, the relative ionization efficiency is rather well defined, if the laser is optimally aligned, but for the metals the determination of RIE is more complex as it seems to be affected by the ratio of metals to rBC. As a consequence, metals present in exhaust particles can be detected with different efficiencies depending on the rBC concentration or they can even be missed if they are externally mixed with rBC or do not absorb laser light themselves. The SP-AMS, similar to the other aerosol mass spectrometers, allows to measure only particles larger than ~40 nm in size, which in regard to the exhaust emission particles implies that a significant fraction of small particles can be neglected.

Overall, the results of this study showed that, although there can be a large variation between individual buses of the same type, the combination of engine, fuel, lubricating oil and after-treatment system produces specific mass spectral signatures. As a consequence, when old diesel buses are replaced by the newer emission standard buses (EEV level) with efficient after-treatment systems and/or alternative fuels, the characteristics of ambient particles in urban areas may change. The differences detected in the composition of organics in this study suggests that for buses the transition from diesel-fueled to hybrid and ethanol buses could result in larger fraction of oxygenated organics in freshly emitted aerosol whereas the increase in CNG buses may change the composition less as organic matter emitted from CNG buses is more similar to that from diesel buses. However, the change in bus fleet has most significant impact on local air quality by decreasing particle mass concentrations.

Acknowledgments

Aleksi Malinen and Kaapo Lindholm from Metropolia and Panu Karjalainen, Anssi Järvinen and Hugo Wihersaari from Tampere University of Technology are acknowledged for their contribution to the chasing experiments by Sniffer.

Funding

This work was supported by the Academy of Finland (Grant No. 259016 and Grant No. 293437) and TEKES in the CLEEN Ltd (the cluster for Energy and Environment) MMEA (Measurement, Monitoring and Environmental Assessment) programme (WP4.5.2).

ORCID

D. Worsnop http://orcid.org/0000-0002-8928-8017

References

Aiken, A. C., Salcedo, D., Cubison, M. J., Huffman, J. A., DeCarlo, P. F., Ulbrich, I. M., Docherty, K. S., Sueper, D., Kimmel, J. R., Worsnop, D. R., Trimborn, A., Northway, M., Stone, E. A., Schauer, J. J., Volkamer, R. M., Fortner, E., de Foy, B., Wang, J., Laskin, A., Shutthanandan, V., Zheng, J., Zhang, R., Gaffney, J., Marley, N. A., Paredes-Miranda, G., Arnott, W. P., Molina, L. T., Sosa, G., and Jimenez, J. L. (2009). Mexico City Aerosol Analysis During MILAGRO using High Resolution Aerosol Mass Spectrometry at the Urban Supersite (T0)—Part 1: Fine Particle Composition and Organic Source Apportionment. *Atmos. Chem. Phys.*, 9:6633–6653.

Al-Qurashi, K., and Boehman, A. L. (2008). Impact of Exhaust Gas Recirculation (EGR) on the Oxidative Reactivity of Diesel Engine Soot. *Combust. Flame*, 155:675–695.

Arnold, F., Pirjola, L., Rönkkö, T., Reichl, U., Schlager, H., Lähde, T., Heikkilä, J., and Keskinen, J. (2012). First on-Line Measurements of Sulfuric Acid Gas in Modern Heavy Duty Diesel Engine Exhaust: Implications for Nanoparticle Formation. *Environ. Sci. Technol.*, 46:11227–11234.

Aurela, M., Saarikoski, S., Niemi, J.V., Canonaco, F., Prévôt, A. S.H., Frey, A., Carbone, S., Kousa, A., and Hillamo, R. (2015). Chemical and Source Characterization of Submicron Particles at Residential and Traffic Sites in the Helsinki Metropolitan Area, Finland. *Aerosol Air Qual. Res.*, 15:1213–1226.

Bockhorn, H. (1994). *Soot formation in combustion, mechanisms and models*. Springer Series in Chemical Physics, Springer-Verlag, Berlin, Vol. 59.

Bruning, I. M. R. A., and Malm, E. B. (1982). Identificação e quantificação das impurezas presentes no etanol [Identification and quantification of impurities present in ethanol]. *Bol. Tec. Petrobrás* 25:217.

Canagaratna, M. R., Jayne, J. T., Ghertner, D. A., Herndon, S., Shi, Q., Jimenez, J. L., Silva, P. J., Williams, P., Lanni, T., Drewnick, F., Demerjian, K. L., Kolb, C. E., and Worsnop, D. R. (2004). Chase Studies of Particulate Emissions from in-use New York City Vehicles. *Aerosol Sci. Technol.*, 38:555–573.

Canagaratna, M. R., Jayne, J. T., Jimenez, J. L., Allan, J. D., Alfarra, M. R., Zhang, Q., Onasch, T. B., Drewnick, F., Coe,

H., Middlebrook, A., Delia, A., Williams, L. R., Trimborn, A. M., Northway, M. J., DeCarlo, P. F., Kolb, C. E., Davidovits, P., and Worsnop, D. R. (2007). Chemical and Microphysical Characterization of Ambient Aerosols with the Aerodyne Aerosol Mass Spectrometer. *Mass Spectrom. Rev.*, 26:185–222.

Carbone, S., Onasch, T., Saarikoski, S., Timonen, H., Saarnio, K., Sueper, D., Rönkkö, T., Pirjola, L., Worsnop, D., and Hillamo, R. (2015). Characterization of Trace Metals with the SP-AMS: Detection and Quantification. *Atmos. Meas. Tech.*, 8:4803–4815.

Chirico, R., DeCarlo, P. F., Heringa, M. F., Tritscher, T., Richter, R., Prévôt, A. S. H., Dommen, J., Weingartner, E., Wehrle, G., Gysel1, M., Laborde, M., and Baltensperger, U. (2010). Impact of Aftertreatment Devices on Primary Emissions and Secondary Organic Aerosol Formation Potential from in-use Diesel Vehicles: Results from Smog Chamber Experiments. *Atmos. Chem. Phys.* 10:11545–11563.

Corbin, J. C., Sierau, B., Gysel, M., Laborde, M., Keller, A., Kim, J., Petzold, A., Onasch, T. B., Lohmann, U., and Mensah, A. A. (2014). Mass Spectrometry of Refractory Black Carbon Particles from Six Sources: Carbon-Cluster and Oxygenated Ions. *Atmos. Chem. Phys.*, 14:2591–2603.

Crippa, M., Canonaco, F., Lanz, V. A., Äijälä, M., Allan, J. D., Carbone, S., Capes, G., Dall'Osto, M., Day, D. A., DeCarlo, P. F., Di Marco, C. F., Ehn, M., Eriksson, A., Freney, E., Hildebrandt Ruiz, L., Hillamo, R., Jimenez, J.-L., Junninen, H., Kiendler-Scharr, A., Kortelainen, A.-M., Kulmala, M., Mensah, A. A., Mohr, C., Nemitz, E., O'Dowd, C., Ovadnevaite, J., Pandis, S. N., Petäjä, T., Poulain, L., Saarikoski, S., Sellegri, K., Swietlicki, E., Tiitta, P., Worsnop, D. R., Baltensperger, U. and Prévôt, A. S. (2014). Organic Aerosol Components Derived from 25 AMS Datasets Across Europe using a Newly Developed ME-2 Based Source Apportionment Strategy. *Atmos. Chem. Phys.*, 14:6159–6176.

Cross, E. S., Sappok, A., Fortner, E. C., Hunter, J. F., Jayne, J. T., Brooks, W. A., Onasch, T. B., Wong, V. W., Trimborn, A., Worsnop, D. R., and Kroll, J. H. (2012). Real-Time Measurements of Engine-Out Trace Elements: Application of a Novel Soot Particle Aerosol Mass Spectrometer for Emissions Characterization. *J. Eng. Gas Turb. Power*, 137:072801.

Dallmann, T. R., Onasch, T. B., Kirchstetter, T. W., Worton, D. R., Fortner, E. C., Herndon, S. C., Wood, E. C., Franklin, J. P., Worsnop, D. R., Goldstein, A. H., and Harley, R. A. (2014). Characterization of Particulate Matter Emissions from On-Road Gasoline and Diesel Vehicles using a Soot Particle Aerosol Mass Spectrometer. *Atmos. Chem. Phys.*, 14:7585–7599.

Gomaa, M., Alimin, A. J., and Kamarudin, K. A. (2010). Trade-off between NOX, Soot and EGR Rates for an IDI Diesel Engine Fuelled with JB5. *Int. J. Mech. Aeros. Indu. Mech. Manuf. Eng.*, 4:196–201.

Johnson, T. (2013). Vehicular Emissions in Review. *SAE Int. J. Engine*, 6:699–715.

Karjalainen, P., Rönkkö, T., Lähde, T., Rostedt, A., Keskinen, J., Saarikoski, S., Aurela, M., Hillamo, R., Malinen, A., Pirjola, L., and Amberla, A. (2012). Reduction of Heavy-Duty Diesel Exhaust Particle Number and Mass at Low Exhaust Temperature Driving by the DOC and the SCR. *SAE Int. J. Fuels Lubr.*, 5, doi:10.4271/2012-01-1664

Kittelson, D. B. (1998). Engines and Nanoparticles: A Review. *J. Aerosol Sci.* 29:575–588.

Kittelson, D. B., Watts, W. F., Johnson, J. P., Thorne, C., Higham, C., Payne, J., Goodier, S., Warrens, C., Preston, H., Zink, U., Pickles, D., Goersmann, C., Twigg, M. V., Walker, A. P., and Boddy, R. (2008). Effect of Fuel and Lube Oil Sulfur on the Performance of a Diesel Exhaust Gas Continuously Regenerating Trap. *Environ. Sci. Technol.*, 42:9276–9282.

Korn, M. D. A., dos Santos, D. S. S., Welz, B., Vale, M. G. R., Teixeira, A. P., Lima, D. D., and Ferreira, S. L.C. (2007). Atomic Spectrometric Methods for the Determination of Metals and Metalloids in Automotive Fuels—A Review. *Talanta*, 73:1–11.

Li, X., Xu, Z., Guan, C., and Huang, Z. (2015). Oxidative Reactivity of Particles Emitted from a Diesel Engine Operating at Light Load with EGR. *Aerosol Sci. Technol.*, 49:1–10.

Lim, Y. B., and Ziemann, P. J. (2009). Effects of Molecular Structure on Aerosol Yields from OH Radical-Initiated Reactions of Linear, Branched, and Cyclic Alkanes in the Presence of Nox. *Environ. Sci. Technol.*, 43:2328–2334.

Lähde, T., Rönkkö, T., Virtanen, A., Schuck, T. J., Pirjola, L., Hämeri, K., Kulmala, M., Arnold, F., Rothe, E., and Keskinen, J. (2009). Heavy Duty Diesel Engine Exhaust Aerosol Particle and Ion Measurements. *Environ. Sci. Technol.*, 43:163–168.

Maricq, M., Chase, R., Xu, N., and Laing, P. (2002). The Effects of the Catalytic Converter and Fuel Sulphur Level on Motor Vehicle Particulate Matter Emissions: Light Duty Diesel Vehicles. *Environ. Sci. Technol.*, 36:283–289.

Mohr, C., Huffman, J. A., Cubison, M. J., Aiken, A. C., Docherty, K. S., Kimmel, J. R., Ulbrich, I. M., Hannigan, M., and Jimenez, J. L. (2009). Characterization of Primary Organic Aerosol Emissions from Meat Cooking, Trash Burning, and Motor Vehicles with High-Resolution Aerosol Mass Spectrometry and Comparison with Ambient and Chamber Observations. *Environ. Sci. Technol.*, 43:2443–2449.

Ng, N. L., Canagaratna, M. R., Jimenez, J. L., Zhang, Q., Ulbrich, I. M., and Worsnop, D. R. (2011). Real-Time Methods for Estimating Organic Component Mass Concentrations from Aerosol Mass Spectrometer Data. *Environ. Sci. Technol.*, 45:910–916.

Nilsson, P. T., Eriksson, E. C., Ludvigsson, L., Messing, M. E., Nordin, E.Z., Gudmundsson, A., Meuller, B. O., Deppert, K., Fortner, E. C., Onasch, T. B., and Pagels, J. H. (2015). In-Situ Characterization of Metal Nanoparticles and their Organic Coatings Using Laser-Vaporization Aerosol Mass Spectrometry. *Nano Res.*, 12:3780–3795.

Nilsson, P. T., Isaxon, C., Eriksson, A. C., Messing, M. E., Ludvigsson, L., Rissler, J., Hedmer, M., Tinnerberg, H., Gudmundsson, A., Deppert, K., Bohgard, M., and Pagels, J. H. (2013). Nano-objects Emitted during Maintenance of Common Particle Generators: Direct Chemical Characterization with Aerosol Mass Spectrometry and Implications for Risk Assessments. *J Nanopart Res.*, 15:2052.

Onasch, T. B., Trimborn, A., Fortner, E. C., Jayne, J. T., Kok, G. L., Williams, L. R., Davidovits, P., and Worsnop, D. R. (2012). Soot Particle Aerosol Mass Spectrometer: Development, Validation, and Initial Application. *Aero. Sci. Technol.*, 46:804–817.

Pakkanen, T. A., Loukkola, K., Korhonen, C. H., Aurela, M., Mäkelä, T., Hillamo, R. E., Aarnio, P., Koskentalo, T., Kousa, A., and Maenhaut, W. (2001). Sources and Chemical Composition of Atmospheric Fine and Coarse Particles in the Helsinki Area. *Atmos. Environ.*, 35:5381–5391.

Pirjola, L., Dittrich, A., Niemi, J. V., Saarikoski, S., Timonen, H., Kuuluvainen, H., Järvinen, A., Kousa, A., Rönkkö, T., and Hillamo, R. (2016). Physical and Chemical Characterization of Real-World Particle Number and Mass Emissions from City Buses in Finland. *Environ. Sci. Technol.*, 50:294–304.

Pirjola, P., Karjalainen, P., Heikkilä, J., Saari, S., Tzamkiozis, T., Ntziachristos, L., Kulmala, K., Keskinen, J., and Rönkkö, T. (2015). Effects of Fresh Lubricant Oils on Particle Emissions Emitted by a Modern Gasoline Direct Injection Passenger Car. *Environ. Sci. Technol.*, 49:3644–3652.

Pirjola, L., Parviainen, H., Hussein, T., Valli, A., Hämeri, K., Aalto, P., Virtanen, A., Keskinen, J., Pakkanen, T., Mäkelä, T., and Hillamo, R.. (2004). "Sniffer"—a novel tool for chasing vehicles and measuring traffic pollutants. *Atmos. Environ.* 38:3625–3635.

Robinson, M. A., Olson, M. R., Liu, Z. G., and Schauer, J. J. (2015). The Effects of Emission Control Strategies on Light-Absorbing Carbon Emissions from a Modern Heavy-Duty Diesel Engine. *J. Air Waste Manag.*, 65:759–766.

Rönkkö, T., Lähde, T., Heikkilä, J., Pirjola, L., Bauschke, U., Arnold, F., Schlager, H., Rothe, D., Yli-Ojanperä, J., and Keskinen, J. (2013). Effect of gaseous sulphuric acid on diesel exhaust nanoparticle formation and characteristics. *Environ. Sci. Technol.*, 47:11882–11889.

Saarikoski, S., Timonen, H., Saarnio, K., Aurela, M., Järvi, L., Keronen, P., Kerminen, V.-M., and Hillamo, R. (2008). Sources of Organic Carbon in PM1 in Helsinki Urban Air. *Atmos. Chem. Phys.*, 8:6281–6295.

Saarnio, K., Niemi, J.V., Saarikoski, S., Aurela, M., Timonen, H., Teinilä, K., Myllynen, M., Frey, A., Lamberg, H., Jokiniemi, J., and Hillamo, R. (2012). Using Monosaccharide Anhydrides to Estimate the Impact Wood Combustion on Fine Particles in the Helsinki Metropolitan area. *Boreal Environ. Res.* 17:163–183.

Salcedo, D., Laskin, A., Shutthanandan, V., and Jimenez, J.-L. (2012). Feasibility of the Detection of Trace Elements in Particulate Matter Using Online High-Resolution Aerosol Mass Spectrometry. *Aerosol Sci. Technol.*, 46:1187–1200.

Sage, A. M., Weitkamp, E. A., Robinson, A. L., and Donahue, N. M. (2007). Evolving Mass Spectra of the Oxidized Component of Organic Aerosol: Results from Aerosol Mass Spectrometer Analyses of Aged Diesel Emissions. *Atmos. Chem. Phys. Discuss.*, 7:10065–10096.

Taylor, D. B., and Synovec, R.E. (1993). Chromatographic Determination of Copper Speciation in Jet Fuel. *Talanta* 40:495–501.

Tobias, H., Beving, D., Ziemann, P., Sakurai, H., Zuk, M., McMurry, P., Zarling, D., Watylonis, R., and Kittelson, D. (2001). Chemical Analysis of Diesel Engine Nanoparticles using a Nano-DMA/Thermal Desorption Particle Beam Mass Spectrometer. *Environ. Sci. Technol.*, 35:2233–2243.

Wang, Y.-F., Huang, K.-L., Li, C,-T., Mi, H.-H., Luo, J.-H., and Tsai, P.-J. (2003). Emissions of Fuel Metals Content from a Diesel Vehicle Engine. *Atmos. Environ.*, 33:4637–4643.

Yawar, W. (2010). Determination of Wear Metals in Lubricating Oils by Flame Atomic Absorption Spectrophotometry. *J. Anal. Chem.*, 65:489–491.

Yu, Z., Herndon, S. C., Ziemba, L. D., Timko, M. T., Liscinsky, D. S., Anderson, B. E., and Miake-Lye, R. C. (2012). Identification of Lubrication Oil in the Particulate Matter Emissions from Engine Exhaust of In-Service Commercial Aircraft. *Environ. Sci. Technol.*, 46:9630−9637.